Kragujevac J. Sci. 45 (2023) 7-14
doi: 10.5937/KgJSci2345007M

UDC 537.531:621.395.721.5/.387.36:617.51
Original scientific paper

ANALYSIS OF SPECIFIC ABSORPTION RATE IN THE HUMAN HEAD MODEL EXPOSED TO RADIOFREQUENCY RADIATION

Marko M. Milošević*, Željko M. Cimbaljević, Milena P. Živković, Nenad D. Stevanović, Vladimir M. Marković, Dragana Z. Krstić

University of Kragujevac, Faculty of Science, Department of Physics, Radoja Domanovića 12, 34000 Kragujevac, Serbia
*****Corresponding author; E-mail: markommmilosevic@gmail.com

(Received April 14, 2023; Accepted May 23, 2023)

ABSTRACT. As mobile phones have become a necessity in modern society, and there is an increasing number of users of various ages, it is imperative to investigate the impact of mobile phone radiofrequency electromagnetic radiation (RF) on humans. Because the human head is one of the most exposed and sensitive organs in the body, this paper investigated the propagation of the electromagnetic (EM) field through it. Additionally, the Specific absorption rate (SAR) was examined to study how RF radiation affects the human head. A program code using the finite-difference time-domain (FDTD) method was created to simulate the propagation of RF radiation through the six layers that make up the human head (skin, fat, bone, dura mater, CSF, and brain). RF radiation at the following frequencies was investigated: 0.9 GHz, 1.8 GHz, 2.4 GHz, 3.35 GHz, and 4.5 GHz. Values of the thickness and parameters of the layers can also be changed in the program. It was discovered that the majority of the EM energy is absorbed in the skin of the human head.

Keywords: electromagnetic radiation, mobile phones, human head, FDTD, SAR.

INTRODUCTION

Radiofrequency (RF) radiation is part of the spectrum of EM waves in the frequency range from 3 kHz to 300 GHz. Sources of RF radiation can be natural or artificial. Atmospheric fields, Earth's electromagnetic field, and cosmic radiation are examples of natural sources. Transmitting antennas from radio and television stations, mobile phone base stations, mobile phones, etc. are examples of artificial sources. The negative effects of mobile phones on the human body are being studied more and more as they have emerged as the most prevalent sources of RF radiation (KESHVARI *et al.*, 2006; AZIZ, 2009; DJORDJEVIC, 2009a, b). There are three types of RF radiation effects: thermal, athermal, and nonthermal (LAK and ORAIZI, 2013). Thermal effects are particularly pronounced and indicate a rise in tissue temperature caused by RF radiation energy absorption, whereas non-thermal effects are faintly expressed and occur on cell membranes and can induce cancer or other DNA and chromosome damage (VALBERG, 1997; WESSAPAN and RATTANADECHO, 2012; KODERA *et al.*, 2018; WUST *et al.*, 2020). The

major world organizations continue to disregard non-thermal effects and base their radiation protection advice on the thermal effect (LWIN and YOKOTA, 2019).

The specific absorption rate (SAR) is a quantity commonly used to assess the influence of RF radiation on biological systems. It represents the absorbed energy of RF radiation per unit of the mass density of the environment and is defined by the relation:

$$SAR = \frac{\sigma E^2}{\rho} \tag{1}$$

where E is the peak amplitude of the electrical field (V/m), σ is the tissue conductivity (S/m), and ρ is the tissue density (kg/m^3). The unit for SAR is W/kg (LWIN and YOKOTA, 2019). SAR estimates can be made using a variety of software: HFSS software (LAK and ORAIZI, 2013), FEKO software (MARY and RAVICHANDRAN, 2013), COMSOL Multiphysics software (GREEN, 2021), etc. Numerous authors conduct SAR analyses using numerical methods such as the finite-difference time-domain (FDTD) method (AKRAM and JASMY, 2008; RAJAGOPAL and RAJASEKARAN, 2014; SABBAH *et al.*, 2011) and finite element method (FEM) (KARANASIOU, 2014). SAR can be determined experimentally in biological systems, for example, by measuring the change in body temperature with a thermal imaging camera (BHAT and KUMAR, 2013), but it is more commonly calculated first and the temperature rise is derived from it (NISHIZAWA and HASHIMOTO, 1999; HIRATA and FUJIWARA, 2009). In this paper, a program was developed to simulate the propagation of RF radiation through a two-dimensional (2D) medium using the FDTD method. That program was used to analyze SAR in the human head, represented by a multi-layered 2D model, with the parameters of the layers depending on the frequency of the RF radiation of the mobile phone to which the model was exposed. The developed program enables precise discretization of model layers and parameter definition, giving more accurate results.

MATERIALS AND METHODS

Application of FDTD methods for propagation of RF radiation

The FDTD method, which employs time-dependent Maxwell's equations in differential form, is one of the simplest methods for solving complex problems in electromagnetism (SULLIVAN, 2013). In this work, the following two Maxwell's equations were used to develop the program (SCHNEIDER, 2022):

$$-\sigma_m \boldsymbol{H} - \mu \frac{\partial \boldsymbol{H}}{\partial t} = \nabla \times \boldsymbol{E}, \tag{2}$$

$$\sigma \mathbf{E} + \varepsilon \frac{\partial \mathbf{E}}{\partial t} = \nabla \times \mathbf{H}. \tag{3}$$

For the transverse electric mode waves, the electric field only has a *z* component, and its value changes along the *x* and *y* axes. The magnetic field is composed of *x* and *y* components that vary along the *x* and *y* axes. Relations (2) and (3) have the following scalar form:

$$-\sigma_{\mathrm{m}} H_{\mathrm{x}} - \mu \frac{\partial H_{\mathrm{x}}}{\partial t} = \frac{\partial E_{\mathrm{z}}}{\partial y}, \tag{4}$$

$$\sigma_{\mathrm{m}} H_{\mathrm{y}} + \mu \frac{\partial H_{\mathrm{y}}}{\partial t} = \frac{\partial E_{\mathrm{z}}}{\partial x}, \tag{5}$$

$$\sigma E_z + \varepsilon \frac{\partial E_z}{\partial t} = \frac{\partial H_y}{\partial x} - \frac{\partial H_x}{\partial y}. \tag{6}$$

Space and time are discretized in the FDTD method. The spatial and time derivatives in Maxwell's equations are replaced by finite differences, yielding equations (4), (5), and (6) in which the electric and magnetic fields in a given time step are expressed as the electric and magnetic fields in the previous time step as (SCHNEIDER, 2022):

$$H_x^{q+\frac{1}{2}}\left[m, n+\frac{1}{2}\right] = \frac{1-\frac{\sigma_m \Delta t}{2\mu}}{1+\frac{\sigma_m \Delta t}{2\mu}} H_x^{q-\frac{1}{2}}\left[m, n+\frac{1}{2}\right] - \frac{1}{1+\frac{\sigma_m \Delta t}{2\mu}} \frac{\Delta t}{\mu \Delta y}\left(E_z^q[m, n+1] - E_z^q[m, n]\right), \tag{7}$$

$$H_y^{q+\frac{1}{2}}\left[m+\frac{1}{2}, n\right] = \frac{1-\frac{\sigma_m \Delta t}{2\mu}}{1+\frac{\sigma_m \Delta t}{2\mu}} H_y^{q-\frac{1}{2}}\left[m+\frac{1}{2}, n\right] + \frac{1}{1+\frac{\sigma_m \Delta t}{2\mu}} \frac{\Delta t}{\mu \Delta x}\left(E_z^q[m+1, n] - E_z^q[m, n]\right), \tag{8}$$

$$E_z^{q+1}[m, n] = \frac{1-\frac{\sigma \Delta t}{2\varepsilon}}{1+\frac{\sigma \Delta t}{2\varepsilon}} E_z^q[m, n] + \frac{1}{1+\frac{\sigma \Delta t}{2\varepsilon}} \frac{\Delta t}{\varepsilon \Delta x}\left(H_y^{q+\frac{1}{2}}\left[m+\frac{1}{2}, n\right] - H_y^{q+\frac{1}{2}}\left[m-\frac{1}{2}, n\right]\right) - \frac{1}{1+\frac{\sigma \Delta t}{2\varepsilon}} \frac{\Delta t}{\varepsilon \Delta y}\left(H_x^{q+\frac{1}{2}}\left[m, n+\frac{1}{2}\right] - H_x^{q+\frac{1}{2}}\left[m, n-\frac{1}{2}\right]\right). \tag{9}$$

In equations (7-9) Δx and Δy represent spatial steps along the *x* and *y* axes, respectively, and Δt is the time step. Numbers m, n and q are integer values that represent the number of steps for Δx, Δy and Δt, respectively. The nodes of the electric field are positioned at integer values of the spatial steps, whereas the nodes of both magnetic field components are shifted by half the spatial step regarding the nodes of the electric field. The electric field exists at times equal to the integer values of the time step, whereas both components of the magnetic field exist at times half a time step later than the electric field. Relations (7), (8), and (9) over matrices can be expressed as follows:

$$H_x[m, n] = C_{hxh}[m, n] H_x[m, n] - C_{hxe}[m, n]\left(E_z[m, n+1] - E_z[m, n]\right), \tag{10}$$

$$H_y[m, n] = C_{hyh}[m, n] H_y[m, n] + C_{hye}[m, n]\left(E_z[m+1, n] - E_z[m, n]\right), \tag{11}$$

$$E_z[m, n] = C_{eze}[m, n] E_z[m, n] + C_{ezh}[m, n]\left(\left(H_y[m, n] - H_y[m-1, n]\right) - \left(H_x[m, n] - H_x[m, n-1]\right)\right) \tag{12}$$

where:

$$C_{hxh}[m,n] = \frac{1-\frac{\sigma_m \Delta t}{2\mu}}{1+\frac{\sigma_m \Delta t}{2\mu}}, \tag{13}$$

$$C_{hxe}[m,n] = \frac{1}{1+\frac{\sigma_m \Delta t}{2\mu}} \frac{\Delta t}{\mu \delta}, \tag{14}$$

$$C_{hyh}[m,n] = \frac{1-\frac{\sigma_m \Delta t}{2\mu}}{1+\frac{\sigma_m \Delta t}{2\mu}}, \tag{15}$$

$$C_{hye}[m,n] = \frac{1}{1+\frac{\sigma_m \Delta t}{2\mu}} \frac{\Delta t}{\mu \delta}, \tag{16}$$

$$C_{eze}[m,n] = \frac{1-\frac{\sigma \Delta t}{2\varepsilon}}{1+\frac{\sigma \Delta t}{2\varepsilon}}, \tag{17}$$

$$C_{ezh}[m,n] = \frac{1}{1+\frac{\sigma \Delta t}{2\varepsilon}} \frac{\Delta t}{\varepsilon \delta}. \tag{18}$$

Here was taken $\Delta x = \Delta y = \delta$. The usage of second-order absorbing border conditions (ABC) was utilized to design a 2D network with a finite number of nodes that acts as if it were infinite (such that as little energy as possible is reflected back into the network's interior) (SCHNEIDER, 2022). To define the electric field at a boundary node at a given instant in ABC's second-order condition, the values of the electric fields at that instant in the two adjacent internal nodes, as well as the values of the electric fields at that boundary node and the two adjacent internal nodes in the previous two-time steps, are required. The electric and magnetic fields in each node of the 2D material environment are calculated for each time step. The previously described procedure allows for the simulation of EM wave propagation through a material medium as well as the calculation of RF radiation-specific absorption rate. In the program, it is possible to specify the frequency, relative dielectric constant, relative magnetic constant, medium conductivity, magnetic conductivity, medium size (number of nodes along the x and y axes), values of space and time steps as well as the number of steps.

Human head model

Many works model the head as a 2D system of concentric circles, with each circle representing a different tissue (SABBAH *et al*., 2011; SALLOMI *et al*., 2018; LWIN and YOKOTA, 2019). Figure 1 depicts a schematic model of the human head, which is composed of six tissues: skin, fat, skull (bones), dura mater, CSF, and brain, with the dimensions of each layer shown in

millimeters. For a given frequency of EM waves, each tissue is distinguished by its relative electrical constant and specific conductivity (Tab. 1). The EM wave strikes the head's surface in the y-axis direction, resulting in an electric field vector in the z-axis direction and a magnetic field vector oscillating in the x-axis direction of the coordinate system (Fig. 1).

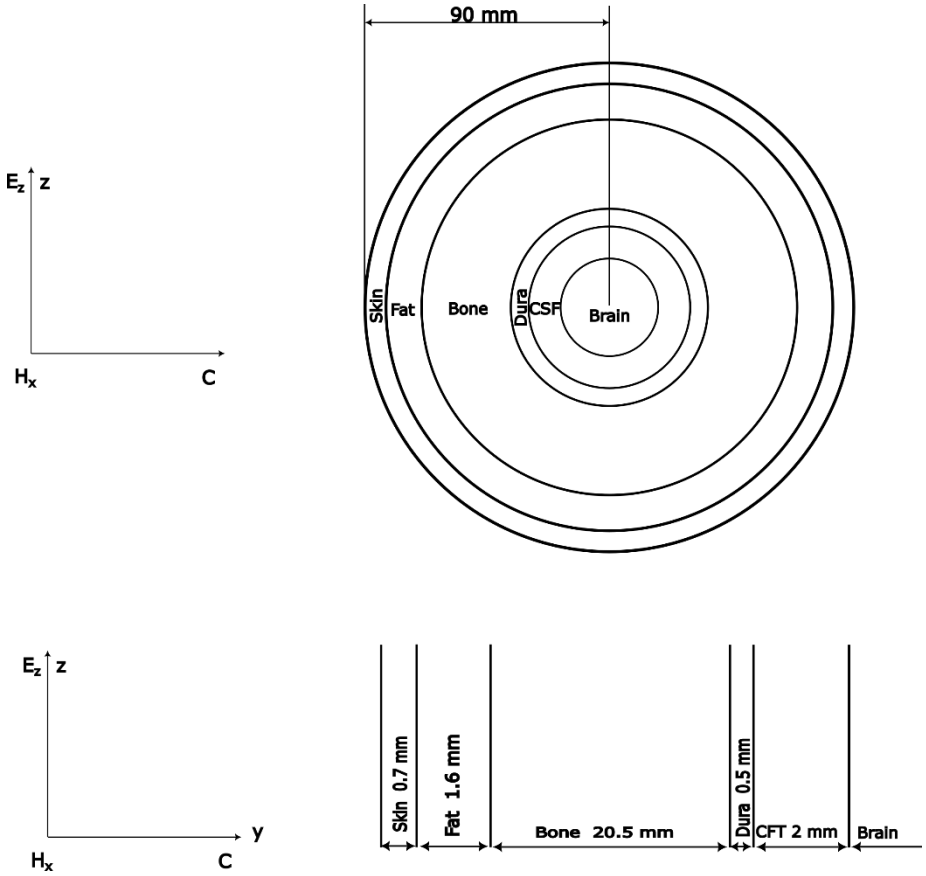

Figure 1. The human head model used for the analysis of SAR.

Table 1. Parameters of layers (tissues) of the human head (LWIN and YOKOTA, 2019; SABBAH *et al*., 2011)

Tissue	Density $\rho\left[kg/m^3\right]$	0.9 GHz		1.8 GHz		2.4 GHz		3.35 GHz		4.45 GHz	
		ε_r	σ [S/m]	ε_r	σ [S/m]	ε_r	σ [S/m]	ε_r	σ [S/m]	ε_r	σ [S/m]
Skin	1100	41.4	0.87	38.9	1.18	38.1	1.44	37.1	1.93	36.18	2.68
Fat	920	5.46	0.05	5.34	0.07	5.29	0.102	5.18	0.14	5.076	0.21
Bone	1850	12.4	0.14	11.8	0.28	11.4	0.38	10.8	0.5	10.28	0.84
Dura	1050	44.4	0.96	42.9	1.32	42.1	1.64	40.9	2.25	39.47	3.15
CSF	1060	68.7	2.41	67.2	2.92	66.3	3.41	64.8	4.39	62.85	5.87
Brain	1030	45.8	0.77	43.5	1.15	42.6	1.48	41.3	2.11	39.91	3.03

To run the simulation, a 2D grid of 340x340 segments was created along the *y* and *z* axes. The size of each spatial segment is equal to $\Delta x = \Delta y = 0.1\,\text{mm}$, and the time step is equal to $\Delta t = \Delta x / 2c_0$. It was assumed that the source is 1 cm away from the head and that the electric field vector changes as $E_z = E_0 \cos(\omega t)$, where ω angular frequency, t is time, and E_0 is the amplitude of the electric field.

RESULTS AND DISCUSSION

Based on the FDTD method described above, a program code was created to simulate the propagation of RF radiation through a human head model. The program code was written in Fortran90 program language. In the program, it is possible to define the frequency of RF radiation, the power, and shape of the source, as well as its distance from the head.

The electric and magnetic fields for each segment of the 2D network of coordinates were calculated iteratively at the initial moment using the set of equations (10)-(12), and then the procedure was repeated in subsequent time intervals, with time step Δt. According to relation (1), the electric field and specific absorption rate of RF radiation in each layer of the head are calculated as a result of the program code for the frequencies 0.9 GHz, 1.8 GHz, 2.4 GHz, 3.35 GHz, and 4.5 GHz. Figure 2 depicts the electric field distribution and the normalized SAR distribution.

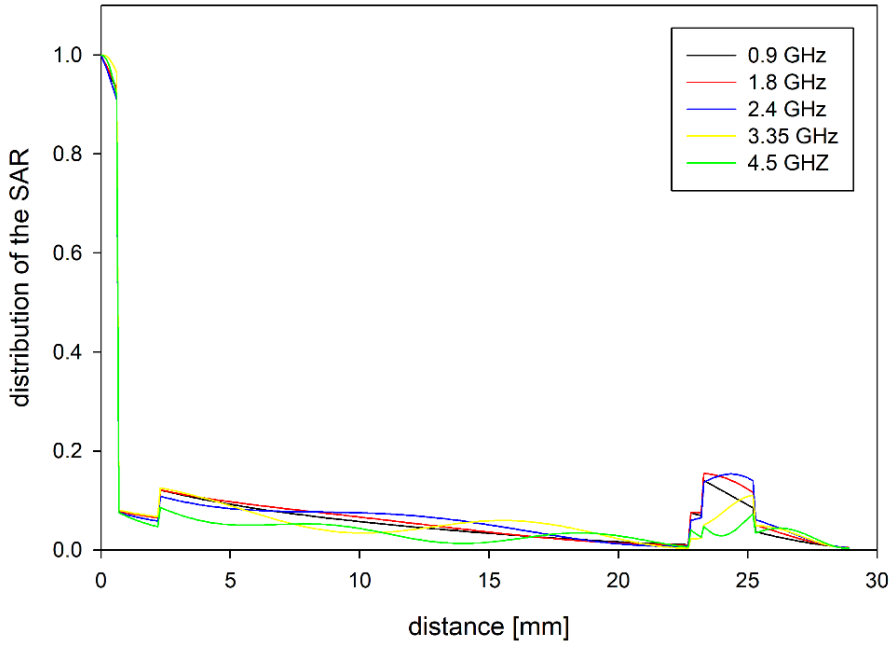

Figure 2. Normalized distribution of the specific absorption rate (SAR) of RF radiation in the head.

Figure 2 shows that the specific absorbed energy of RF radiation is greatest in the skin layer for all frequencies considered. The specific absorbed energy is significantly lower in the deeper layers and decreases with the depth of penetration. The CSF layer, which is located in front of the brain and has significantly higher conductivity than the other layers, is an exception. It can also be seen that the absorbed energy decreases as the radiation frequency increases. These results are in good agreement with the results obtained by (SABBAH *et al.*, 2011; ABDULRAZZAQ and AZIZ, 2013; LWIN and YOKOTA, 2019).

CONCLUSION

The FDTD approach makes it simple to calculate the specific absorbed energy of RF radiation in biological systems. The developed program is applicable to all human organ geometry: a model of concentric spheres (model of head), a model of axial cylinders (model of trunk, arms, and legs), etc. This approach makes it possible to evaluate the deposited energy in all organs of the human body and determine the health risk of using devices with RF radiation sources in them. This research sheds light on which EM radiation frequencies pose the greatest

health risks as different devices use different frequencies. The highest frequencies are less of a health risk because they are less absorbed and penetrate only superficially, whereas the lowest frequencies are more absorbed and penetrate deeper. It is safe to assume that from this perspective, RF radiation poses a negligible health risk to the human head since very little RF radiation penetrates the brain layer for all frequencies. More research should be done to determine how much of a health risk there is from prolonged exposure of the human head to RF radiation sources.

Acknowledgments

This work was supported by the Ministry of Science, Technological Development and Innovation of the Republic of Serbia N_0 451-03-47/2023-01/ 200122.

References:

[1] ABDULRAZZAQ, S.A., AZIZ, J.S. (2013): SAR Simulation in Human Head Exposed to RF Signals and Safety Precautions. *International Journal of Computer Science Engineering and Technology* **3** (9): 334–340.

[2] AKRAM, G., JASMY, Y. (2008): Specific absorption rate (SAR) on the human head as a function of the orientation of plane wave radiation: FDTD-based analysis. *Proceedings - 2nd Asia International Conference on Modelling and Simulation*, AMS 2008, 959–962. doi: 10.1109/AMS.2008.193.

[3] AZIZ, J. (2009): Analysis of Biological Effects of Microwave Energy and Safe Distance Calculations. *Journal of Al-Rafidain Un. For Sciences* 25: 1–14. doi: 10.55562/jrucs.v 25i2.435

[4] BHAT, M.A., KUMAR, V. (2013): Calculation of SAR and measurement of temperature change of the human head due to the mobile phone waves at frequencies 900 MHz and 1800 MHz. *Advances in Physics Theories and Applications* 16: 54–63.

[5] DJORDJEVIC, A. (2009a): Basics of electrical engineering, part 1 Electrostatics. Academic thought. [in Serbian]

[6] DJORDJEVIC, A. (2009b): Basics of electrical engineering, part 3 Electromagnetism. Academic thought. [in Serbian]

[7] GREEN, S. (2021): Computational Model of the Influence of an 835 MHz Patch Antenna Distance on Specific Absorption Rate (SAR) and Temperature Change in the Human Head. *15th I@Q Conference Proceedings.* Inquiry at Queen's Undergraduate Research Conference Proceedings is Queen's University Library's. doi: 10.24908/iqurcp.14573

[8] HIRATA, A., FUJIWARA, O. (2009): The correlation between mass-averaged SAR and temperature elevation in the human head model exposed to RF near-fields from 1 to 6 GHz. *Physics in Medicine and Biology* **54** (23): 7227–7238. doi: 10.1088/0031-9155/54/23/013.

[9] KARANASIOU, I. (2014): SAR estimation in human head models related to TETRA, GSM and UMTS exposure using different computational approaches. *WSEAS Transactions on Biology and Biomedicine* **11**: 101–110

[10] KESHVARI, J., KESHVARI, R., LANG, S. (2006): The effect of increase in dielectric values on specific absorption rate (SAR) in eye and head tissues following 900, 1800 and 2450

MHz radio frequency (RF) exposure. *Physics in Medicine and Biology* **51** (6): 1463–1477. doi: 10.1088/0031-9155/51/6/007

[11] KODERA, S., GOMEZ-TAMES, J., HIRATA, A. (2018): Temperature elevation in the human brain and skin with thermoregulation during exposure to RF energy. *BioMedical Engineering Online* **17**: 1. doi: 10.1186/s12938-017-0432-x

[12] LAK, A., ORAIZI, H. (2013): Evaluation of SAR distribution in six-layer human head model. *International Journal of Antennas and Propagation*, ID 580872 doi: 10.1155/2013/580 87.

[13] LWIN, Z.M., YOKOTA, M. (2019): Numerical analysis of SAR and temperature distribution in two dimensional human head model based on FDTD parameters and the polarization of electromagnetic wave. AEU - *International Journal of Electronics and Communications* **104**: 91–98. doi: 10.1016/j.aeue.2019.03.010

[14] MARY, T.A.J., RAVICHANDRAN, C.S. (2013): Effect of SAR on human head modeling inside cylindrical enclosures. *Electromagnetic Biology and Medicine* **32** (3): 382–389. doi: 10.3109/15368378.2012.728551

[15] NISHIZAWA, S., HASHIMOTO, O. (1999): Effectiveness analysis of lossy dielectric shields for a three-layered human model. IEEE *Transactions on Microwave Theory and Techniques* **47** (3): 277–283. doi: 10.1109/22.750223

[16] RAJAGOPAL, B., RAJASEKARAN, L. (2014): SAR assessment on three layered spherical human head model irradiated by mobile phone antenna. *Human-Centric Computing and Information Sciences* **4** (1): 1–11. doi: 10.1186/s13673-014-0010-1.

[17] SABBAH, A.I., DIB, N.I., AL-NIMR, M.A. (2011): Evaluation of specific absorption rate and temperature elevation in a multi-layered human head model exposed to radio frequency radiation using the finite-difference time domain method. IET *Microwaves, Antennas and Propagation* **5** (9): 1073–1080. doi: 10.1049/iet-map.2010.0172

[18] SALLOMI, A.H., HASHIM, S.A., WALI, M.H. (2018): SAR and thermal effect prediction in human head exposed to cell phone radiations. *Science International (Lahore)* **30** (4): 653–656.

[19] SCHNEIDER, J.B. (2022): Understanding the Finite-Difference Time-Domain Method. Available at: https://eecs.wsu.edu/~schneidj/ufdtd/ufdtd.pdf

[20] SULLIVAN, D.M. (2013): Electromagnetic Simulation Using the FDTD Method. The Institute of Electrical and Electronics Engineers, Inc., New York. doi: 10.1002/ 9781118646700 Available at: http://www.astrosen.unam.mx/~aceves/Fisica_ Computacional/ebooks/sullivan_emsimulation_fdtd.pdf Accessed 20 May 2023.

[21] VALBERG, P.A. (1997): Radio frequency radiation (RFR): the nature of exposure and carcinogenic potential. *Cancer Causes and Control* **8** (3): 323–332. doi: 10.1023/A:10 18449003394

[22] WESSAPAN, T., RATTANADECHO, P. (2012): Numerical analysis of specific absorption rate and heat transfer in human head subjected to mobile phone radiation: Effects of user age and radiated power. *Journal of Heat Transfer* **134** (12): 121101. doi: 10.1115/1.4006595

[23] WUST, P., KORTÜM, B., STRAUSS, U., NADOBNY, J., ZSCHAECK, S., BECK, M., STEIN, U., GHADJAR, P. (2020): Non-thermal effects of radiofrequency electromagnetic fields. *Scientific Reports* **10** (1): 13488. doi: 10.1038/s41598-020-69561-3